

## Chapter 5

# A high order robust adaptive numerical method for singularly perturbed parabolic reaction-diffusion problems

Singularly perturbed parabolic reaction-diffusion problems are a frequently studied class in literature. However, from the literature review we notice that the parameter-robust convergence of high order on layer-adaptive equidistributed meshes is missing. To fill this gap, in this chapter, we present an adaptive numerical method with parameter-robust convergence of order four in space and of order one in time.

Let the domain be  $\bar{G} = G \cup \partial G$ , where  $G := G_x \times (0, T]$  with  $G_x = (0, 1)$ . Suppose  $\partial G = \Gamma_b \cup \Gamma_r \cup \Gamma_l$  with  $\Gamma_b = [0, 1] \times \{0\}$ ,  $\Gamma_l = \{0\} \times (0, T]$ , and  $\Gamma_r = \{1\} \times (0, T]$ . On this domain we define the model problem as follows

$$\begin{cases} \mathcal{L}y := \frac{\partial y}{\partial t} + \mathcal{L}_\varepsilon y = f & \text{for } (x, t) \in G, \\ y(x, 0) = \rho(x) & \text{for } x \in \bar{G}_x, \\ y(0, t) = y(1, t) = 0 & \text{for } t \in (0, T], \end{cases} \quad (5.1)$$

where

$$\mathcal{L}_\varepsilon y := -\varepsilon \frac{\partial^2 y}{\partial x^2} + by,$$

$0 < \varepsilon \ll 1$  is the perturbation parameter, functions  $b$  and  $f$  are sufficiently smooth satisfying  $0 < \beta \leq b(x)$ ,  $x \in \bar{G}_x$ . Under these sufficient smoothness and compatibility conditions, problem (5.1) has a unique solution [5, 34]. Moreover, we have the following bounds [132]

$$\left| \frac{\partial^{p+s} y}{\partial x^p \partial t^s}(x, t) \right| \leq C \left( 1 + \varepsilon^{-\frac{p}{2}} \left( e^{-x\sqrt{\frac{\beta}{\varepsilon}}} + e^{-(1-x)\sqrt{\frac{\beta}{\varepsilon}}} \right) \right), \quad 0 \leq p + 2s \leq 6, \quad p, s \in \mathbb{N}_0. \quad (5.2)$$

In this chapter, we propose a high order adaptive numerical method combining the implicit Euler scheme in time and a non-monotone finite difference scheme in space. We construct the adaptive mesh in space using equidistribution of the monitor function, and a uniform mesh in time. We use two-step discretization of the continuous problem, in which firstly the problem is discretized in time on a uniform mesh using the implicit Euler method to get the linear stationary differential equations in space. Then in the second step these equations are discretized on the non-uniform equidistribution mesh using a non-monotone finite difference scheme. This two-step discretization technique helps us to analyse the error contribution of time and space discretizations separately. The method is proved to be convergent of order one in time and four in space. Further, we use the Richardson extrapolation technique to improve the order of convergence in time from one to two. At the end, the method is implemented on three test examples to validate the theoretical result.

This chapter is organized as follows: In Section 5.1, we consider the time semidiscretization of (5.1). In Section 5.2, the construction of layer-adaptive equidistribution mesh is discussed. Section 5.3 is devoted to the spatial discretization of the time semidiscretized problem. In Section 5.4, the totally discrete scheme is given and the convergence results are combined for both time and space discretizations. Numerical results are given for three test problems in Section 5.5. Section 5.6 concludes the main outcomes of the chapter.

## 5.1 The time semidiscretization

We consider a uniform mesh in time defined by  $\{t_n = n\Delta t, n = 0, \dots, M\}$  with time-step  $\Delta t = \frac{T}{M}$  and discretize the differential equation in problem (5.1) in time using implicit Euler scheme as follows

$$\frac{y^{n+1}(x) - y^n(x)}{\Delta t} + \mathcal{L}_\varepsilon y^{n+1}(x) = f(x, t_{n+1}). \quad (5.3)$$

Thus, we can rewrite (5.1) as a system of ordinary differential equations in space variable  $x$  for each time level  $t_{n+1}$ ,  $n = 0, \dots, M - 1$ , as

$$\left\{ \begin{array}{l} y^0(x) = \rho(x), \\ \text{For } n = 0, \dots, M - 1, \\ \left\{ \begin{array}{l} (I + \Delta t \mathcal{L}_\varepsilon) y^{n+1}(x) = y^n(x) + \Delta t f(x, t_{n+1}), \quad x \in G_x, \\ y^{n+1}(0) = 0, y^{n+1}(1) = 0, \end{array} \right. \end{array} \right. \quad (5.4)$$

where  $I$  is the identity operator. Its solution gives the semidiscrete approximation  $y^{n+1}(x)$  to the exact solution  $y(x, t)$  of (5.1) at the time level  $t_{n+1}$ ,  $n = 0, \dots, M - 1$ . Now for the operator  $(I + \Delta t \mathcal{L}_\varepsilon)$ , we have

$$\|(I + \Delta t \mathcal{L}_\varepsilon)^{-1}\|_{\bar{G}_x} \leq \frac{1}{1 + \beta \Delta t}. \quad (5.5)$$

It follows that the semidiscrete scheme satisfies a discrete maximum principle; thus ensuring the stability of the semidiscrete problem (5.4). Now, for the semidiscrete problem (5.4), we define the local truncation error  $e_{n+1} = y(x, t_{n+1}) - \hat{y}^{n+1}(x)$ , with

$\hat{y}^{n+1}(x)$  being the solution of the auxiliary problem

$$\begin{cases} (I + \Delta t \mathcal{L}_\varepsilon) \hat{y}^{n+1}(x) = y(x, t_n) + \Delta t f(x, t_{n+1}), \\ \hat{y}^{n+1}(0) = 0, \hat{y}^{n+1}(1) = 0. \end{cases} \quad (5.6)$$

*Lemma 5.1.1.* If

$$\left| \frac{\partial^p y(x, t)}{\partial t^p} \right| \leq C, \quad (x, t) \in \bar{G}, \quad 0 \leq p \leq 2,$$

then the local error satisfies

$$\|e_{n+1}\|_{\bar{G}_x} \leq C \Delta t^2.$$

*Proof.* From the above equation (5.6), we have

$$(I + \Delta t \mathcal{L}_\varepsilon) \hat{y}^{n+1}(x) - \Delta t f(x, t_{n+1}) = y(x, t_n).$$

Since the solution  $y$  of (5.1) is sufficiently smooth, we have

$$\begin{aligned} y(x, t_n) &= y(x, t_{n+1}) + \Delta t \mathcal{L}_\varepsilon y(x, t_{n+1}) - \Delta t f(x, t_{n+1}) + \int_{t_n}^{t_{n+1}} (t_n - s) \frac{\partial^2 y(x, s)}{\partial t^2} ds \\ &= (I + \Delta t \mathcal{L}_\varepsilon) y(x, t_{n+1}) - \Delta t f(x, t_{n+1}) + O(\Delta t^2). \end{aligned}$$

Therefore, the local error  $e_{n+1}$  satisfies

$$\begin{aligned} (I + \Delta t \mathcal{L}_\varepsilon) e_{n+1} &= O(\Delta t^2), \\ e_{n+1}(0) &= e_{n+1}(1) = 0. \end{aligned}$$

Now the required result follows using (5.5). □

To prove the uniform convergence of (5.4), we define the global error  $E_n = y(x, t_n) - y^n(x)$  associated with (5.4). Hence,  $E_n = e_n + RE_{n-1}$ , where  $R \equiv (I + \Delta t \mathcal{L}_\varepsilon)^{-1}$  is defined as follows:  $RE_{n-1}$  is obtained with one step of (5.4) taking  $y^n = E_{n-1}$  and  $f$  to be zero. Thus, we get

$$E_n = \sum_{i=1}^n R^{n-i} e_i.$$

Using the stability estimate (5.5), the transition operator  $R$  satisfies

$$\|R^i\|_{\bar{G}_x} \leq C, \quad i = 1, \dots, n. \quad (5.7)$$

Thus, we have the following lemma.

*Lemma 5.1.2.* The global error satisfies

$$\sup_{n\Delta t \leq T} \|E_n\|_{\bar{G}_x} \leq C\Delta t.$$

Next, we recall the solution estimates for the semidiscrete problem (5.6) that we shall require for the error analysis of the spatial discretization in the upcoming sections

$$\left| \frac{d^p \hat{y}^{n+1}(x)}{dx^p} \right| \leq C \left( 1 + \varepsilon^{-\frac{p}{2}} \left( e^{-x\sqrt{\frac{\beta}{\varepsilon}}} + e^{-(1-x)\sqrt{\frac{\beta}{\varepsilon}}} \right) \right), \quad 0 \leq p \leq 6. \quad (5.8)$$

Also, the solution of the semidiscrete problem is decomposed as the regular and singular components [85]:

$$\hat{y}^{n+1}(x) = \hat{v}^{n+1}(x) + \hat{w}^{n+1}(x). \quad (5.9)$$

These components satisfy the following bounds

$$\left| \frac{d^p \hat{v}^{n+1}(x)}{dx^p} \right| \leq C(1 + \varepsilon^{\frac{4-p}{2}}), \quad 0 \leq p \leq 6, \quad (5.10)$$

and

$$\left| \frac{d^p \hat{w}^{n+1}(x)}{dx^p} \right| \leq C e^{-\frac{p}{2}} \left( e^{-x\sqrt{\frac{B}{\varepsilon}}} + e^{-(1-x)\sqrt{\frac{B}{\varepsilon}}} \right), \quad 0 \leq p \leq 6, \quad x \in \bar{G}_x. \quad (5.11)$$

## 5.2 Mesh equidistribution

We generate the layer-adaptive equidistributed mesh with the help of a monitor function. We choose a monitor function that involves the derivatives of the singular component of the solution. Also, we notice from (5.2), that the width and location of the boundary layers do not change in the time direction. Therefore, it is suitable to generate the adaptive mesh at some fixed time level  $0 \leq t_* \leq T$ , and use it for all the time levels. We consider

$$\mathcal{M}(y(x, t_*), x) = \alpha_* + \left| \frac{\partial^2 w}{\partial x^2}(x, t_*) \right|^{1/4}, \quad (5.12)$$

where the positive constant  $\alpha_*$  is chosen so that some mesh points are assured external to boundary layer regions. A spatial mesh  $\bar{G}_x^N := \{0 = x_0 < x_1 < \dots < x_N = 1\}$  is said to equidistribute the monitor function  $\mathcal{M}(y(x, t_*), x)$  if

$$\int_{x_{i-1}}^{x_i} \mathcal{M}(y(x, t_*), x) dx = \int_{x_i}^{x_{i+1}} \mathcal{M}(y(x, t_*), x) dx, \quad 1 \leq i \leq N-1.$$

Alternatively, mesh equidistribution can be seen as a mapping defined from the computational coordinates  $\zeta \in [0, 1]$  to the physical coordinates  $x \in [0, 1]$  given by

$$\int_0^{x(\zeta)} \mathcal{M}(y(x, t_*), x) dx = \zeta \int_0^1 \mathcal{M}(y(x, t_*), x) dx. \quad (5.13)$$

For the analysis purpose we approximate the second order derivative of  $w$  from (5.11) as

$$\frac{\partial^2 w}{\partial x^2}(x, t_\star) \approx \begin{cases} \frac{\chi_1}{\varepsilon} e^{-x\sqrt{\frac{\beta}{\varepsilon}}}, & x \in [0, 1/2], \\ \frac{\chi_2}{\varepsilon} e^{-(1-x)\sqrt{\frac{\beta}{\varepsilon}}}, & x \in (1/2, 1], \end{cases}$$

where  $\chi_1$  and  $\chi_2$  are constants, independent of  $\varepsilon$  and  $x$ . Hence,

$$\int_0^1 \left| \frac{\partial^2 w}{\partial x^2}(x, t_\star) \right|^{1/4} dx \equiv \mathbf{K} \approx 4\varepsilon^{1/4} \left[ \frac{|\chi_1|^{1/4} + |\chi_2|^{1/4}}{\beta^{1/4}} \right].$$

Using the approximate value of  $\frac{\partial^2 w}{\partial x^2}(x, t_\star)$ , equidistribution of (5.12), for  $x(\xi) \leq \frac{1}{2}$  gives

$$\zeta \left( \frac{\alpha_\star}{\mathbf{K}} + 1 \right) = \frac{\alpha_\star}{\mathbf{K}} x(\zeta) + \lambda_1 \left( 1 - e^{-\frac{x(\zeta)}{4}\sqrt{\frac{\beta}{\varepsilon}}} \right), \quad (5.14)$$

where

$$\lambda_1 = \frac{|\chi_1|^{1/4}}{|\chi_1|^{1/4} + |\chi_2|^{1/4}}.$$

Similarly, for  $x(\zeta) > \frac{1}{2}$ , equidistribution gives

$$(1 - \zeta) \left( \frac{\alpha_\star}{\mathbf{K}} + 1 \right) = \frac{\alpha_\star}{\mathbf{K}} (1 - x(\zeta)) + \lambda_2 \left( 1 - e^{-\frac{1-x(\zeta)}{4}\sqrt{\frac{\beta}{\varepsilon}}} \right), \quad (5.15)$$

where

$$\lambda_2 = \frac{|\chi_2|^{1/4}}{|\chi_1|^{1/4} + |\chi_2|^{1/4}}.$$

A non-uniform mesh in physical coordinates  $\{x_i\}_{i=0}^N$  corresponds to an equispaced mesh  $\{\zeta_i = i/N\}_{i=0}^N$  in computational coordinates. So, equations (5.14) and (5.15) can be written as

$$\frac{i}{N} \left( \frac{\alpha_\star}{\mathbf{K}} + 1 \right) = \frac{\alpha_\star}{\mathbf{K}} x_i + \lambda_1 \left( 1 - e^{-\frac{x_i}{4}\sqrt{\frac{\beta}{\varepsilon}}} \right) \quad (5.16)$$

and

$$\left( 1 - \frac{i}{N} \right) \left( \frac{\alpha_\star}{\mathbf{K}} + 1 \right) = \frac{\alpha_\star}{\mathbf{K}} (1 - x_i) + \lambda_2 \left( 1 - e^{-\frac{(1-x_i)}{4}\sqrt{\frac{\beta}{\varepsilon}}} \right) \quad (5.17)$$

Hence, the equidistributed mesh points  $x_i$ 's are given by the solution of the non-linear algebraic equations (5.16) and (5.17). We assume  $\sqrt{\varepsilon} \ll N^{-1}$ , as otherwise a uniform mesh could be used and a classical convergence analysis could be given. The following lemmas provide some important properties of the mesh structure.

*Lemma 5.2.1.* The non-uniform mesh generated by (5.16) and (5.17) on taking  $\alpha_* = \mathbf{K}$  satisfies

$$x_l < 4\sqrt{\frac{\varepsilon}{\beta}} \log N < x_{l+1} \quad \text{and} \quad x_{r-1} < 1 - 4\sqrt{\frac{\varepsilon}{\beta}} \log N < x_r,$$

where

$$l = \left\lceil \frac{1}{2} \left( 4\sqrt{\frac{\varepsilon}{\beta}} N \log N + \lambda_1(N-1) \right) \right\rceil, \quad r = \left\lfloor N - \frac{1}{2} \left( 4\sqrt{\frac{\varepsilon}{\beta}} N \log N + \lambda_2(N-1) \right) \right\rfloor + 1,$$

and  $\lceil \cdot \rceil$  denotes the integer part. Moreover, the mesh spacing satisfies

$$h_i < C\sqrt{\frac{\varepsilon}{\beta}} \quad \text{for } i = 1, \dots, l-1 \text{ and } i = r+1, \dots, N-1,$$

with

$$|h_{i+1} - h_i| \leq Ch_i^2 \quad \text{for } i = 1, \dots, l-1 \quad \text{and} \quad |h_{i+1} - h_i| \leq Ch_{i+1}^2 \quad \text{for } i = r+1, \dots, N.$$

*Proof.* The proof follows from [56]. □

*Lemma 5.2.2.* The mesh widths of equidistributed mesh satisfy  $h_i \leq CN^{-1}$ , for  $i = 1, \dots, N$ .



*Proof.* From (5.12), we have that  $\mathbf{K} = \alpha_* \leq \mathcal{M}(y(x, t_*), x)$ . Now from derivative estimates (5.11), we have

$$\int_0^1 \mathcal{M}(y(x, t_*), x) dx \leq C\varepsilon^{1/4}.$$

Thus, by the equidistribution principle, we get

$$\alpha_* h_i \leq \int_{x_{i-1}}^{x_i} \mathcal{M}(y(x, t_*), x) dx = \frac{1}{N} \int_0^1 \mathcal{M}(y(x, t_*), x) dx \leq C\varepsilon^{1/4} N^{-1}.$$

Hence,  $h_i \leq CN^{-1}$ . □

## 5.3 The spatial discretization and error analysis

In this section, we first introduce a non-monotone high order scheme to discretize problem (5.6) in spatial direction. Then we discuss the stability and error analysis of the spatial discretization.

### 5.3.1 The discretization strategy

We represent the time discretization scheme (5.6) as follows:

$$\begin{cases} \tilde{\mathcal{L}}_\varepsilon \hat{y}^{n+1}(x) = \tilde{f}^{n+1}(x), & x \in G_x \\ \hat{y}^{n+1}(0) = 0, & \hat{y}^{n+1}(1) = 0, \end{cases} \quad (5.18)$$

where

$$\tilde{\mathcal{L}}_\varepsilon = (I + \Delta t \mathcal{L}_\varepsilon) = -\varepsilon \Delta t \frac{d^2}{dx^2} + \tilde{b}(x)I,$$

$$\tilde{b}(x) = (1 + b(x)\Delta t) \quad \text{and} \quad \tilde{f}^{n+1}(x) = (y(x, t_n) + \Delta t f(x, t_{n+1})).$$

Suppose a non-uniform spatial mesh  $\bar{G}_x^N = \{x_i\}_{i=0}^N$  is considered to discretize the domain  $\bar{G}_x$  with mesh width  $h_i = x_i - x_{i-1}$ ,  $i = 1, \dots, N$  and  $\bar{h}_i = (h_i + h_{i+1})/2$ ,  $i = 1, \dots, N - 1$ . The discrete scheme is defined by

$$\begin{cases} [\tilde{L}_{\varepsilon, N} \hat{Y}^{n+1}]_i = -\varepsilon \Delta t \delta_x^2 \hat{Y}_i^{n+1} + \Gamma[\tilde{b} \hat{Y}^{n+1}]_i = \Gamma[\tilde{f}^{n+1}]_i & \text{for } i = 1, \dots, N - 1, \\ \hat{Y}_0^{n+1} = 0, \quad \hat{Y}_N^{n+1} = 0. \end{cases} \quad (5.19)$$

where

$$\begin{aligned} \delta_x^2 \hat{Y}_i^{n+1} &= \frac{1}{\bar{h}_i} \left( \frac{\hat{Y}_{i+1}^{n+1} - \hat{Y}_i^{n+1}}{h_{i+1}} - \frac{\hat{Y}_i^{n+1} - \hat{Y}_{i-1}^{n+1}}{h_i} \right), \\ \Gamma[\tilde{b} \hat{Y}^{n+1}]_i &= \nu_i^- \tilde{b}_{i-1} \hat{Y}_{i-1}^{n+1} + \nu_i^c \tilde{b}_i \hat{Y}_i^{n+1} + \nu_i^+ \tilde{b}_{i+1} \hat{Y}_{i+1}^{n+1}, \\ \text{and } \Gamma[\tilde{f}^{n+1}]_i &= \nu_i^- \tilde{f}_{i-1}^{n+1} + \nu_i^c \tilde{f}_i^{n+1} + \nu_{i+1}^+ \tilde{f}_{i+1}^{n+1}, \end{aligned}$$

with 
$$\nu^- = \frac{2h_i - h_{i+1}}{12h_i}, \quad \nu^c = \frac{5}{6}, \quad \nu^+ = \frac{2h_{i+1} - h_i}{12h_i}.$$

### 5.3.2 Stability of scheme (5.19)

Note that the discrete operator  $\tilde{L}_{\varepsilon, N}$  is not inverse monotone. Therefore, for the proof of stability of scheme (5.19), we shall follow the idea used in [133] for a different scheme. On an arbitrary non-uniform spatial mesh  $\bar{G}_x^N$  with maximal step size  $h_{max}$ , we consider another discrete operator  $[\Lambda_{\varepsilon, N}]$  defined by

$$[\Lambda_{\varepsilon, N} \hat{Y}^{n+1}]_i := -\varepsilon \Delta t \delta_x^2 \hat{Y}_i^{n+1} - \frac{h_{i+1}}{12\bar{h}_i} \tilde{b}_i \hat{Y}_{i-1}^{n+1} + \frac{5}{6} \tilde{b}_i \hat{Y}_i^{n+1} - \frac{h_i}{12\bar{h}_i} \tilde{b}_i \hat{Y}_{i+1}^{n+1}. \quad (5.20)$$

The matrix corresponding to the operator  $\Lambda_{\varepsilon, N}$  has positive entries on the diagonal and non-positive entries on off-diagonal with row sum  $\frac{2}{3} \tilde{b}_i > 0$ . Therefore, it is an  $M$ -matrix and satisfies the following comparison principle.

*Lemma 5.3.1.* Let  $\psi^{n+1}$  and  $\phi^{n+1}$  be two mesh functions that satisfy  $[\Lambda_{\varepsilon,N}\psi^{n+1}]_i \geq [\Lambda_{\varepsilon,N}\phi^{n+1}]_i$  for  $i = 1, \dots, N-1$ ,  $\psi_0^{n+1} \geq \phi_0^{n+1}$  and  $\psi_N^{n+1} \geq \phi_N^{n+1}$ , then  $\psi_i^{n+1} \geq \phi_i^{n+1}$  for  $i = 0, \dots, N$ .

Dividing (5.20) by  $\tilde{b}_i$ , we obtain an  $M$ -matrix with row sum  $2/3$ . Thus, we obtain

$$\|\psi^{n+1}\|_{\bar{G}_x^N} \leq \frac{3}{2} \left\| \frac{\Lambda_{\varepsilon,N}\psi^{n+1}}{\tilde{b}} \right\|_{\bar{G}_x^N}, \quad (5.21)$$

for all mesh functions  $\psi^{n+1}$  with  $\psi_0^{n+1} = \psi_N^{n+1} = 0$ . This result will be used to establish the stability of the operator  $\tilde{L}_{\varepsilon,N}$  as given in the following theorem.

*Theorem 5.3.1.* Let  $\kappa \in (0, 1)$  be an arbitrary but fixed number. Then, the following stability estimate holds

$$\|\psi^{n+1}\|_{\bar{G}_x^N} \leq \frac{3}{1-\kappa} \left\| \frac{\tilde{L}_{\varepsilon,N}\psi^{n+1}}{\tilde{b}} \right\|_{\bar{G}_x^N}$$

for any mesh function  $\psi^{n+1}$  with  $\psi_0^{n+1} = \psi_N^{n+1} = 0$ , provided  $h_{max}$  is bounded by some threshold value that is independent of  $\varepsilon$ .

*Proof.* Let  $\psi^{n+1}$  be an arbitrary mesh function with  $\psi_0^{n+1} = \psi_N^{n+1} = 0$ . Then, on using (5.19) and (5.20), we can write

$$[\Lambda_{\varepsilon,N}\psi^{n+1}]_i = [\tilde{L}_{\varepsilon,N}\psi^{n+1}]_i - \frac{h_{i+1}}{12\tilde{h}_i} \tilde{b}_{i-1} \psi_{i-1}^{n+1} - \frac{h_i}{12\tilde{h}_i} \tilde{b}_i \psi_{i+1}^{n+1} - \nu_i^- \tilde{b}_{i-1} \psi_{i-1}^{n+1} - \nu_i^+ \tilde{b}_{i+1} \psi_{i+1}^{n+1}.$$

Further simplifications give

$$\begin{aligned} [\Lambda_{\varepsilon,N}\psi^{n+1}]_i &= [\tilde{L}_{\varepsilon,N}\psi^{n+1}]_i - \frac{h_i}{6\tilde{h}_i} \tilde{b}_{i-1} \psi_{i-1}^{n+1} - \frac{h_{i+1}}{6\tilde{h}_i} \tilde{b}_{i+1} \psi_{i+1}^{n+1} + \frac{h_i}{12\tilde{h}_i} (\tilde{b}_{i+1} - \tilde{b}_i) \psi_{i+1}^{n+1} \\ &\quad + \frac{h_{i+1}}{12\tilde{h}_i} (\tilde{b}_{i-1} - \tilde{b}_i) \psi_{i-1}^{n+1}. \end{aligned}$$

Thus,

$$|[\Lambda_{\varepsilon,N}\psi^{n+1}]_i| \leq |[\tilde{L}_{\varepsilon,N}\psi^{n+1}]_i| + \left( \frac{h_{i+1}\tilde{b}_{i+1} + h_i\tilde{b}_{i-1}}{6\tilde{h}_i} + \frac{h_i|\tilde{b}_{i+1} - \tilde{b}_i| + h_{i+1}|\tilde{b}_{i-1} - \tilde{b}_i|}{12\tilde{h}_i} \right) \times \|\psi^{n+1}\|_{\bar{G}_x^N}.$$

Now using equation (5.21), we have

$$\begin{aligned} \|\psi^{n+1}\|_{\bar{G}_x^N} &\leq \frac{3}{2} \left\| \frac{\tilde{L}_{\varepsilon,N}\psi^{n+1}}{\tilde{b}} \right\|_{\bar{G}_x^N} \\ &+ \frac{3}{2} \|\psi^{n+1}\|_{\bar{G}_x^N} \max_{i=1,\dots,N-1} \left( \frac{h_{i+1}\tilde{b}_{i+1} + h_i\tilde{b}_{i-1}}{6\tilde{b}_i\tilde{h}_i} + \frac{h_i|\tilde{b}_{i+1} - \tilde{b}_i| + h_{i+1}|\tilde{b}_{i-1} - \tilde{b}_i|}{12\tilde{b}_i\tilde{h}_i} \right) \end{aligned} \quad (5.22)$$

As  $b$  is sufficiently smooth, there exists a constant  $\gamma$  such that  $|b(z_1) - b(z_2)| \leq \gamma|z_2 - z_1|$ , for all  $z_1, z_2 \in [0, 1]$ . Consequently,

$$\frac{h_{i+1}\tilde{b}_{i+1} + h_i\tilde{b}_{i-1}}{6\tilde{b}_i\tilde{h}_i} + \frac{h_i|\tilde{b}_{i+1} - \tilde{b}_i| + h_{i+1}|\tilde{b}_{i-1} - \tilde{b}_i|}{12\tilde{b}_i\tilde{h}_i} \leq \frac{1}{3} + \frac{\gamma h_{max}}{3\beta} \leq \frac{1 + \kappa}{3},$$

provided  $h_{max}$  is bounded by a value that is independent of  $\varepsilon$ . Thus, from (5.22), we have

$$\|\psi^{n+1}\|_{\bar{G}_x^N} \leq \frac{3}{2} \left\| \frac{\tilde{L}_{\varepsilon,N}\psi^{n+1}}{\tilde{b}} \right\|_{\bar{G}_x^N} + \frac{1 + \kappa}{2} \|\psi^{n+1}\|_{\bar{G}_x^N}. \quad (5.23)$$

Hence, the theorem follows from (5.23). □

### 5.3.3 Error analysis

Now we discuss error analysis of the spatial discretization scheme on non-uniform equidistributed meshes. Suppose  $\eta = \hat{y}^{n+1} - \hat{Y}^{n+1}$  denotes the error of the spatial

discretization and it can be decomposed into the sum of two parts  $\eta = \psi + \phi$ , where  $\psi, \phi \in \mathbb{R}_0^{N+1} \equiv \{\gamma \in \mathbb{R}^{N+1} : \gamma_0 = \gamma_N = 0\}$  and satisfy

$$[\tilde{L}_{\varepsilon,N}\eta]_i = \varepsilon\Delta t \left[ \Gamma \left[ \frac{d^2 \hat{y}^{n+1}}{dx^2} \right] - \delta_x^2 \hat{y}^{n+1} \right]_i, \quad i = 1, \dots, N-1,$$

and

$$[\Lambda_{\varepsilon,N}\eta]_i = [\Lambda_{\varepsilon,N}\psi]_i + [\Lambda_{\varepsilon,N}\phi]_i, \quad i = 1, \dots, N-1,$$

where

$$[\Lambda_{\varepsilon,N}\psi]_i = [\tilde{L}_{\varepsilon,N}\eta]_i$$

and

$$[\Lambda_{\varepsilon,N}\phi]_i = -\frac{h_{i+1}}{12\tilde{h}_i} \tilde{b}_i \eta_{i-1} - \frac{h_i}{12\tilde{h}_i} \tilde{b}_i \eta_{i+1} - \nu_i^- \tilde{b}_{i-1} \eta_{i-1} - \nu_i^+ \tilde{b}_{i+1} \eta_{i+1}.$$

Let  $\kappa \in (0, 1)$  be arbitrary, but fixed. Using the arguments as in Theorem 5.3.1, we have

$$|[\Lambda_{\varepsilon,N}\phi]_i| \leq \frac{(1+\kappa)}{3} \tilde{b}_i \|\eta\|_{\bar{G}_x^N} \quad \text{for } i = 1, \dots, N-1,$$

provided  $N$  is greater than some threshold value that is independent of  $\varepsilon$ . Then the stability result gives

$$\|\phi\|_{\bar{G}_x^N} \leq \frac{(1+\kappa)}{2} \|\eta\|_{\bar{G}_x^N}.$$

On applying the triangle inequality we obtain

$$\|\eta\|_{\bar{G}_x^N} \leq \|\psi\|_{\bar{G}_x^N} + \|\phi\|_{\bar{G}_x^N} \leq \|\psi\|_{\bar{G}_x^N} + \frac{(1+\kappa)}{2} \|\eta\|_{\bar{G}_x^N}.$$

Thus, we obtain the bound on the error in terms of  $\psi$  as follows

$$\|\hat{y}^{n+1} - \hat{Y}^{n+1}\|_{\bar{G}_x^N} \leq \frac{2}{(1-\kappa)} \|\psi\|_{\bar{G}_x^N}. \quad (5.24)$$

Now we estimate  $\|\psi\|$  by using the truncation error and the barrier function technique. The truncation error of scheme (5.19) can be obtained by using the Taylor expansions. We have

$$|[\Lambda_{\varepsilon, N}\psi]_i| = |[\tilde{L}_{\varepsilon, N}\eta]_i| = \varepsilon\Delta t \left| \left[ \Gamma \left[ \frac{d^2 \hat{y}^{n+1}}{dx^2} \right] - \delta_x^2 \hat{y}^{n+1} \right]_i \right|, \quad i = 1, \dots, N-1.$$

Now according to the decomposition of  $\hat{y}^{n+1}$ , we can split the truncation error as

$$\begin{aligned} & \varepsilon\Delta t \left| \left[ \Gamma \left[ \frac{d^2 \hat{y}^{n+1}}{dx^2} \right] - \delta_x^2 \hat{y}^{n+1} \right]_i \right| \\ & \leq \varepsilon\Delta t \left| \left[ \Gamma \left[ \frac{d^2 \hat{v}^{n+1}}{dx^2} \right] - \delta_x^2 \hat{v}^{n+1} \right]_i \right| + \varepsilon\Delta t \left| \left[ \Gamma \left[ \frac{d^2 \hat{w}^{n+1}}{dx^2} \right] - \delta_x^2 \hat{w}^{n+1} \right]_i \right|, \end{aligned} \quad (5.25)$$

and estimate the local truncation errors separately for the regular and singular components. Firstly, for the regular component, we have

$$\begin{aligned} \varepsilon\Delta t \left| \left[ \Gamma \left[ \frac{d^2 \hat{v}^{n+1}}{dx^2} \right] - \delta_x^2 \hat{v}^{n+1} \right]_i \right| & \leq C\varepsilon\Delta t \left[ (h_{i+1} - h_i)^2 \left| \frac{d^4 \hat{v}_i^{n+1}}{dx^4} \right| \right. \\ & \quad \left. + (h_{i+1}^2 + h_i^2) |h_{i+1} - h_i| \left| \frac{d^5 \hat{v}_i^{n+1}}{dx^5} \right| + (h_{i+1}^4 + h_i^4) \max_{x_{i-1} \leq x \leq x_{i+1}} \left| \frac{d^6 \hat{v}^{n+1}(x)}{dx^6} \right| \right], \end{aligned}$$

which on using the bounds on derivatives of  $\hat{v}^{n+1}$  from (5.10) and Lemma 5.2.2 gives

$$\varepsilon\Delta t \left| \left[ \Gamma \left[ \frac{d^2 \hat{v}^{n+1}}{dx^2} \right] - \delta_x^2 \hat{v}^{n+1} \right]_i \right| \leq C\varepsilon\Delta t N^{-2} + C\sqrt{\varepsilon}\Delta t N^{-3} + C\Delta t N^{-4}.$$

Then from the assumption  $N^{-1} \gg \sqrt{\varepsilon}$ , it follows that

$$\varepsilon\Delta t \left| \left[ \Gamma \left[ \frac{d^2 \hat{v}^{n+1}}{dx^2} \right] - \delta_x^2 \hat{v}^{n+1} \right]_i \right| \leq C\Delta t N^{-4}. \quad (5.26)$$

Next, for the singular component, the analysis is done in two parts: inside and outside the boundary layer regions. Firstly, for outside the boundary layers i.e. for

$i = l, \dots, r$ , for some  $\theta_i \in (x_{i-1}, x_{i+1})$ , we have

$$\begin{aligned} \varepsilon \Delta t \left| \left[ \Gamma \left[ \frac{d^2 \hat{w}^{n+1}}{dx^2} \right] - \delta_x^2 \hat{w}^{n+1} \right]_i \right| &= \varepsilon \Delta t \left| \left( \nu_i^- \frac{d^2 \hat{w}_{i-1}^{n+1}}{dx^2} + \nu_i^c \frac{d^2 \hat{w}_i^{n+1}}{dx^2} + \nu_i^+ \frac{d^2 \hat{w}_{i+1}^{n+1}}{dx^2} \right) \right. \\ &\quad \left. - \frac{d^2 \hat{w}^{n+1}(\theta_i)}{dx^2} \right| \\ &\leq \varepsilon \Delta t \max_{x_{i-1} \leq x \leq x_{i+1}} \left| \frac{d^2 \hat{w}^{n+1}(x)}{dx^2} \right| (|\nu_i^-| + \nu_i^c + |\nu_i^+|) \\ &\leq C \varepsilon \Delta t \varphi_i \max_{x_{i-1} \leq x \leq x_{i+1}} \left| \frac{d^2 \hat{w}^{n+1}(x)}{dx^2} \right|, \end{aligned}$$

where

$$\varphi_i = \begin{cases} 1 - 2\nu_i^-, & \text{if } 2h_i \leq 2h_{i+1}, \\ 1 - 2\nu_i^+, & \text{if } 2h_i > 2h_{i+1} \text{ and } \nu_i^+ < 0, \\ 1, & \text{if } 2h_i > 2h_{i+1} \text{ and } \nu_i^+ > 0. \end{cases}$$

It is easy to see that  $\varphi_i \leq C$ ; hence

$$\varepsilon \Delta t \left| \left[ \Gamma \left[ \frac{d^2 \hat{w}^{n+1}}{dx^2} \right] - \delta_x^2 \hat{w}^{n+1} \right]_i \right| \leq C \varepsilon \Delta t \max_{x_{i-1} \leq x \leq x_{i+1}} \left| \frac{d^2 \hat{w}}{dx^2}(x, t_{n+1}) \right|.$$

Now using bound (5.11), we get

$$\varepsilon \Delta t \left| \left[ \Gamma \left[ \frac{d^2 \hat{w}^{n+1}}{dx^2} \right] - \delta_x^2 \hat{w}^{n+1} \right]_i \right| \leq C \Delta t \begin{cases} e^{-x_{i-1} \sqrt{\frac{\beta}{\varepsilon}}}, & x_i \leq \frac{1}{2}, \\ e^{-(1-x_{i+1}) \sqrt{\frac{\beta}{\varepsilon}}}, & x_i > \frac{1}{2}. \end{cases}$$

When  $l \leq i$  and  $x_i \leq \frac{1}{2}$ ,

$$\varepsilon \Delta t \left| \left[ \Gamma \left[ \frac{d^2 \hat{w}^{n+1}}{dx^2} \right] - \delta_x^2 \hat{w}^{n+1} \right]_i \right| \leq C \Delta t \left( e^{-\frac{x_{l-1}}{4} \sqrt{\frac{\beta}{\varepsilon}}} \right)^4.$$

Now, from the mesh equidistribution condition (5.16), we have

$$\begin{aligned} e^{-\frac{x_{l-1}}{4}\sqrt{\frac{\beta}{\varepsilon}}} &= \frac{1}{\lambda_1} \left( x_{l-1} + \lambda_1 - \frac{2(l-1)}{N} \right) \\ &\leq \left( 4\sqrt{\frac{\varepsilon}{\beta}} \log N + \lambda_1 - \frac{1}{N} \left( \lambda_1(N-1) + 4\sqrt{\frac{\varepsilon}{\beta}} \log N - 4 \right) \right) \\ &\leq CN^{-1}. \end{aligned}$$

Therefore, for  $l \leq i$  and  $x_i \leq \frac{1}{2}$ , we obtain

$$\varepsilon \Delta t \left| \left[ \Gamma \left[ \frac{d^2 \hat{w}^{n+1}}{dx^2} \right] - \delta_x^2 \hat{w}^{n+1} \right]_i \right| \leq C \Delta t N^{-4}.$$

Again, the same bound can be obtained by giving the similar argument for  $i \leq r$  and  $x_i > \frac{1}{2}$ . Thus, for  $i = l, \dots, r$ ,

$$\varepsilon \Delta t \left| \left[ \Gamma \left[ \frac{d^2 \hat{w}^{n+1}}{dx^2} \right] - \delta_x^2 \hat{w}^{n+1} \right]_i \right| \leq C \Delta t N^{-4}. \quad (5.27)$$

Now, inside the boundary layers i.e. for  $n = 0, \dots, M-1$ ,  $i = 1, \dots, l-1$  and for  $i = r+1, \dots, N-1$ , we have

$$\begin{aligned} \varepsilon \Delta t \left| \left[ \Gamma \left[ \frac{d^2 \hat{w}^{n+1}}{dx^2} \right] - \delta_x^2 \hat{w}^{n+1} \right]_i \right| &\leq C \varepsilon \Delta t \left[ (h_{i+1} - h_i)^2 \left| \frac{d^4 \hat{w}_i^{n+1}}{dx^4} \right| + (h_{i+1}^2 + h_i^2) |h_{i+1} - h_i| \right. \\ &\quad \left. \times \left| \frac{d^5 \hat{w}_i^{n+1}}{dx^5} \right| + (h_{i+1}^4 + h_i^4) \max_{x_{i-1} \leq x \leq x_{i+1}} \left| \frac{d^6 \hat{w}^{n+1}(x)}{dx^6} \right| \right] \\ &\leq C \Delta t \left[ h_i^4 \varepsilon^{-1} e^{-x_i \sqrt{\frac{\beta}{\varepsilon}}} + h_i^4 \varepsilon^{-3/2} e^{-x_i \sqrt{\frac{\beta}{\varepsilon}}} + h_i^4 \varepsilon^{-2} e^{-x_i \sqrt{\frac{\beta}{\varepsilon}}} \right] \\ &\leq C \Delta t \varepsilon^{-2} h_i^4 e^{-x_i \sqrt{\frac{\beta}{\varepsilon}}}, \end{aligned}$$

where we have used the fact that

$$e^{-x_{i-1} \sqrt{\frac{\beta}{\varepsilon}}} = e^{-x_i \sqrt{\frac{\beta}{\varepsilon}}} e^{h_i \sqrt{\frac{\beta}{\varepsilon}}} \leq C e^{-x_i \sqrt{\frac{\beta}{\varepsilon}}}, \quad \text{using Lemma 5.2.1.}$$



Now, using the equidistribution principle, it holds

$$\begin{aligned} h_i^4 e^{-\sqrt{\frac{\beta}{\varepsilon}} x_i} &\leq \left( \int_{x_{i-1}}^{x_i} e^{-\frac{x}{4} \sqrt{\frac{\beta}{\varepsilon}}} dx \right)^4 \leq \left( \varepsilon^{\frac{1}{4}} \int_{x_{i-1}}^{x_i} \mathcal{M}(y(x, t_\star), x) dx \right)^4 \\ &\leq C\varepsilon \mathbf{K}^4 N^{-4} \leq C\varepsilon^2 N^{-4}. \end{aligned}$$

Hence, we get

$$\varepsilon \Delta t \left| \left[ \Gamma \left[ \frac{d^2 \hat{w}^{n+1}}{dx^2} \right] - \delta_x^2 \hat{w}^{n+1} \right]_i \right| \leq C \Delta t N^{-4}. \quad (5.28)$$

On combining the various bounds for the truncation errors from (5.26)-(5.28) with (5.25), we obtain

$$|[\Lambda_{\varepsilon, N} \psi]_i| = |[\tilde{L}_{\varepsilon, N} \eta]_i| = \varepsilon \Delta t \left| \left[ \Gamma \left[ \frac{d^2 \hat{y}^{n+1}}{dx^2} \right] - \delta_x^2 \hat{y}^{n+1} \right]_i \right| \leq C \Delta t N^{-4}. \quad (5.29)$$

Combine (5.29) with the stability result 5.21 to obtain

$$\|\psi\|_{\bar{G}_x^N} \leq C \Delta t N^{-4}. \quad (5.30)$$

Hence, using (5.30) in (5.24) we obtain

$$\|\hat{y}^{n+1} - \hat{Y}^{n+1}\|_{\bar{G}_x^N} \leq C \Delta t N^{-4}.$$

Thus, we have the following theorem.

*Theorem 5.3.2.* Let  $\hat{y}^{n+1}$  be the exact solution of (5.6) and  $\hat{Y}^{n+1}$  be its numerical approximation using (5.19) on the equidistributed mesh (5.16)-(5.17). Then the following error estimate holds

$$\|\hat{y}^{n+1} - \hat{Y}^{n+1}\|_{\bar{G}_x^N} \leq C \Delta t N^{-4}.$$

## 5.4 The total discretization scheme

Now we combine the time semidiscretization process with the spatial semidiscretization process to obtain the total discretization scheme for computing the approximate solution of (5.1). Let  $Y_i^n$  be the numerical approximations to  $y(x_i, t_n)$ , for  $n = 0, \dots, M$ , and  $i = 0, \dots, N$ . The discretization scheme is given as

$$\begin{cases} Y_i^0 = \rho_i, \quad i = 0, \dots, N, \\ [L_N^M Y]_i^{n+1} := Q[Y_i^{n+1}] = \Gamma[\tilde{f}_i^{n+1}], \quad i = 1, \dots, N-1, \quad n = 0, \dots, M-1, \\ Y_0^{n+1} = 0, \quad Y_N^{n+1} = 0, \quad n = 0, \dots, M-1, \end{cases} \quad (5.31)$$

where  $\tilde{f}_i^{n+1} = Y_i^n + \Delta t f(x_i, t_{n+1})$  and  $\tilde{b}_i = 1 + \Delta t b(x_i)$ . Here,  $Q$  and  $\Gamma$  are the discretization operators given as

$$Q[Y_i^{n+1}] = q_i^- Y_{i-1}^{n+1} + q_i^c Y_i^{n+1} + q_i^+ Y_{i+1}^{n+1}, \quad \Gamma[\tilde{f}_i^{n+1}] = \nu_i^- \tilde{f}_{i-1}^{n+1} + \nu_i^c \tilde{f}_i^{n+1} + \nu_i^+ \tilde{f}_{i+1}^{n+1},$$

where

$$q_i^- = -\frac{\varepsilon \Delta t}{h_i \tilde{h}_i} + \nu_i^- \tilde{b}_{i-1}, \quad q_i^c = \frac{2\varepsilon \Delta t}{h_{i+1} h_i} + \nu_i^c \tilde{b}_i, \quad q_i^+ = -\frac{\varepsilon \Delta t}{h_{i+1} \tilde{h}_i} + \nu_i^+ \tilde{b}_{i+1},$$

$$\nu_i^- = \frac{2h_i - h_{i+1}}{12\tilde{h}_i}, \quad \nu_i^c = \frac{5}{6}, \quad \nu_i^+ = \frac{2h_{i+1} - h_i}{12\tilde{h}_i},$$

with

$$h_i = x_i - x_{i-1} \quad \text{and} \quad \tilde{h}_i = \frac{h_i + h_{i+1}}{2}.$$

Now we conclude this section with the following main theorem.

*Theorem 5.4.1.* Let  $y$  be the exact solution of (5.1) and  $Y^n$  be its numerical approximation obtained using the totally discrete scheme (5.31) at time level  $t_n$ . Then the global error at time level  $t_n$  satisfies

$$\|y(x_i, t_n) - Y_i^n\|_{\bar{G}_x^N} \leq C(\Delta t + N^{-4}).$$

*Proof.* Suppose  $E_n^N = y(x_i, t_n) - Y_i^n$ ,  $e_n^N = y(x_i, t_n) - \hat{y}^n(x_i)$  and  $d_n^N = \hat{y}^n(x_i) - \hat{Y}^n(x_i)$ . Then

$$E_n^N = e_n^N + d_n^N + R_N E_{n-1}^N,$$

where  $R_N$  is the transition operator associated to the totally discrete scheme (5.31).  $R_N V$  is the application of one step of the totally discrete scheme (5.31), with  $Y^n = V$  and zero source term  $f$ . From the above recurrence relation, we obtain the following inequality

$$\|E_n^N\|_{\bar{G}_x^N} \leq \sum_{j=1}^n \|R_N^{n-j}\|_{\bar{G}_x^N} (\|e_j^N\|_{\bar{G}_x^N} + \|d_j^N\|_{\bar{G}_x^N}).$$

Now taking into account that the powers of the transition operator of the totally discrete scheme  $R_N^j$  preserve the uniform boundedness behaviour (due to the stability result) as observed for  $R^j$ , it follows that

$$\begin{aligned} \|E_n^N\|_{\bar{G}_x^N} &\leq C \sum_{j=1}^n ((\Delta t)^2 + \Delta t N^{-4}) \\ &\leq C(\Delta t + N^{-4}). \end{aligned}$$

□

## 5.5 Numerical results

In this section, we perform some numerical experiments to verify the theoretical error bound obtained in the previous section. Firstly the equidistributed mesh is generated at a specific time level by using the De Boor algorithm [47]. Then, in the second step, the adaptive solution is found on this mesh at each time step. The maximum pointwise errors and the corresponding rates of convergence are calculated by using the known solution or by using the double mesh principle if the exact solution is not available. For the test problems, we shall observe the influence of the discretization parameters in space and time on the maximum error and rate of convergence. The numerical observations are given in the form of tables and figures. In our numerical experiments the equidistributed mesh is generated at the time level  $t_1$  and we have taken  $\varrho_0 = 1.1$  as stopping criterion in the algorithm. The smooth component  $V_i^n$  is approximated by

$$\begin{cases} V_i^0 = \rho_i, & i = 0, \dots, N, \\ (1 + \Delta t b(x_i))V_i^{n+1} = V_i^n + \Delta t f(x_i, t_{n+1}), & i = 0, \dots, N, \quad n = 0, \dots, M - 1. \end{cases} \quad (5.32)$$

### Richardson extrapolation

We can further improve the theoretically proved first order rate of convergence in time by using the Richardson extrapolation technique in time. We set the extrapolated solution  $(Y_i^{n+1})_{ext}$  as

$$(Y_i^{n+1})_{ext} = 2Y_{2,i}^{n+1} - Y_{1,i}^{n+1}, \quad (5.33)$$

where  $Y_{1,i}^{n+1}$  and  $Y_{2,i}^{n+1}$  are the solutions of the totally discrete scheme (5.31) with time step sizes  $\Delta t = T/M$  and  $\Delta t = T/2M$ , respectively.

---

**Algorithm 4:** Numerical algorithm for the adaptive mesh and adaptive solution

---

**Input:**  $N, M \in \mathbb{N}$ ,  $0 < \varepsilon \leq 1$  and  $\varrho > 1$ .

**Output:** Adaptive mesh  $\{x_i\}$  and adaptive solution  $Y_i^n$  at the time level  $t_n$ .

1. Initialise the mesh iterations  $\{x_i^{(r)}\}$  with  $r = 0$  as the uniform mesh for  $n = 1$ .
2. Solve the discrete problem (5.31) for  $Y_i^{n,(r)}$ , and (5.32) for  $V_i^{n,(r)}$  on  $\{x_i^{(r)}\}$  and compute  $W_i^{n,(r)} = Y_i^{n,(r)} - V_i^{n,(r)}$ .
3. Find  $\mathcal{M}_i^{(r)} = \alpha^{(r)} + |\delta_x^2 W_i^{n,(r)}|^{1/4}$ ,  $i = 1, \dots, N - 1$  where  $\alpha^{(r)}$  is defined by

$$\alpha^{(r)} = h_1^{(r)} |\delta_x^2 W_1^{n,(r)}|^{1/4} + \sum_{i=2}^{N-1} h_i^{(r)} \left\{ \frac{|\delta_x^2 W_{i-1}^{n,(r)}|^{1/4} + |\delta_x^2 W_i^{n,(r)}|^{1/4}}{2} \right\} + h_N^{(r)} |\delta_x^2 W_{N-1}^{n,(r)}|^{1/4}.$$

4. Set  $H_i^{(r)} = \left( \frac{\mathcal{M}_{i-1}^{(r)} + \mathcal{M}_i^{(r)}}{2} \right) h_i^{(r)}$ ,  $i = 1, \dots, N$ , with  $\mathcal{M}_0^{(r)} = \mathcal{M}_1^{(r)}$  and  $\mathcal{M}_N^{(r)} = \mathcal{M}_{N-1}^{(r)}$ . Then define  $B_i$  by  $B_i = \sum_{j=1}^i H_j^{(r)}$  for  $i = 1, \dots, N$  and  $B_0 = 0$ .
  5. **Stopping criterion:** Choose a constant  $\varrho_0 > 1$  defined by  $\varrho^{(r)} = \frac{N}{B_N} \max_{i=1, \dots, N} H_i^{(r)}$ . If  $\varrho^{(r)} \leq \varrho_0$  then go to Step 7, else continue with Step 6.
  6. Define  $Z_i = i \frac{B_N}{N}$ ,  $i = 0, \dots, N$ . Generate a new mesh  $\{x_i^{(r+1)}\}$  by evaluating the interpolant of  $(B_i, x_i^{(r)})$  at the points  $Z_i$  and return to Step 2 setting  $r = r + 1$ .
  7. Take  $\{x_i^{(r)}\}$  as the layer-adaptive mesh  $\{x_i\}$  for all time levels and  $Y_i^{n,(r)}$  as the required adaptive solution  $Y_i^n$  at the time level  $n = 1$ .
  8. Use the spatial mesh  $\{x_i\}$  at each time level and solve (5.31) to compute the adaptive solution  $Y_i^n$  for  $n = 2, 3, \dots, M$ .
-

### 5.5.1 Numerical experiments

*Example 5.5.1.* Consider the problem [88]

$$\begin{cases} \frac{\partial y}{\partial t} - \varepsilon \frac{\partial^2 y}{\partial x^2} + (1 + xe^{-t})y = f(x, t), & (x, t) \in G, \\ y(x, 0) = 0, \quad x \in \bar{G}_x, \quad y(0, t) = 0, \quad y(1, t) = 0, \quad t \in (0, T], \end{cases} \quad (5.34)$$

with the term  $f(x, t)$  defined according to the known solution

$$y(x, t) = (1 - e^{-t}) \left( \frac{e^{\frac{-x}{\sqrt{\varepsilon}}} + e^{\frac{-(1-x)}{\sqrt{\varepsilon}}}}{1 + e^{\frac{-1}{\sqrt{\varepsilon}}}} - \cos^2(\pi x) \right).$$

Figure 5.1 displays the numerical solution of Example 5.5.1 for  $\varepsilon = 10^{-5}$ , from which

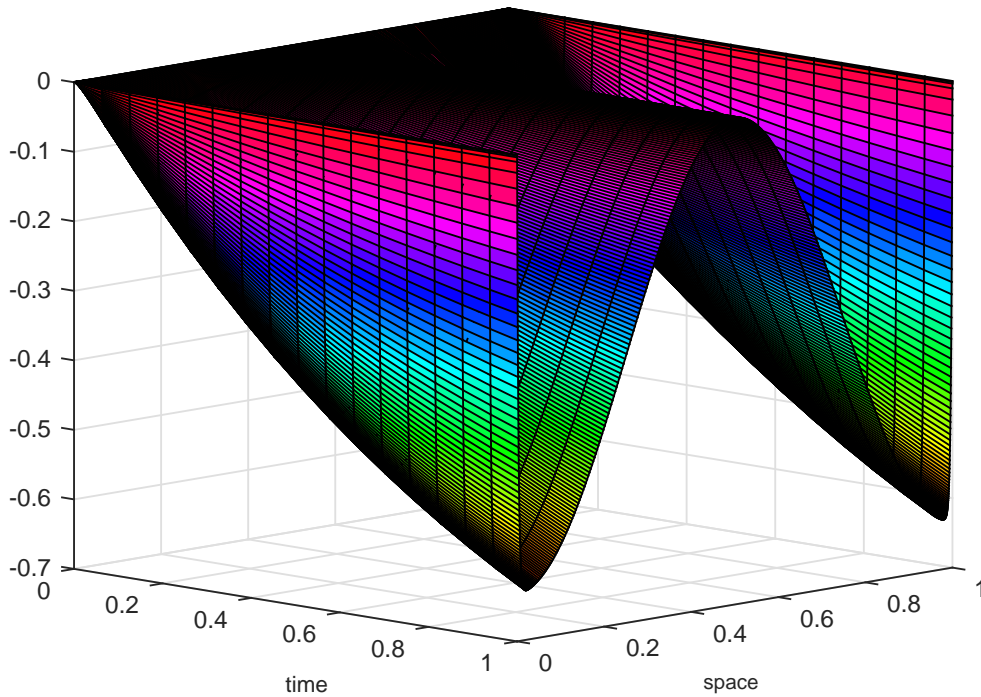


FIGURE 5.1: Surface plot of numerical solution of Example 5.5.1 for  $\varepsilon = 10^{-5}$ ,  $N = 512$  and  $M = 16$

we can clearly observe the boundary layers at both the ends  $x = 0$  and  $x = 1$ . For different values of  $\varepsilon$ ,  $N$  and  $M$ , we calculate the pointwise errors by

$$E_{i,n}^{\varepsilon,N,M} = |\bar{Y}_i^n - y(x_i, t_n)|,$$

where  $\bar{Y}_i^n = Y_i^n$  (if scheme 5.31 is used) or  $\bar{Y}_i^n = (Y_i^n)_{ext}$  (if scheme (5.31) is used with the extrapolation technique (5.33)). Using these values the maximum errors and the numerical rates of convergence are computed by the formulas

$$E^{\varepsilon,N,M} = \max_{i,n} E_{i,n}^{\varepsilon,N,M}, \quad F^{\varepsilon,N,M} = \log_2 \left( \frac{E^{\varepsilon,N,M}}{E^{\varepsilon,2N,2M}} \right).$$

Finally, the parameter-robust errors and the parameter-robust rates of convergence over the set of values of  $\varepsilon$  are obtained by

$$E^{N,M} = \max_{\varepsilon} E^{\varepsilon,N,M}, \quad F^{N,M} = \log_2 \left( \frac{E^{N,M}}{E^{2N,2M}} \right).$$

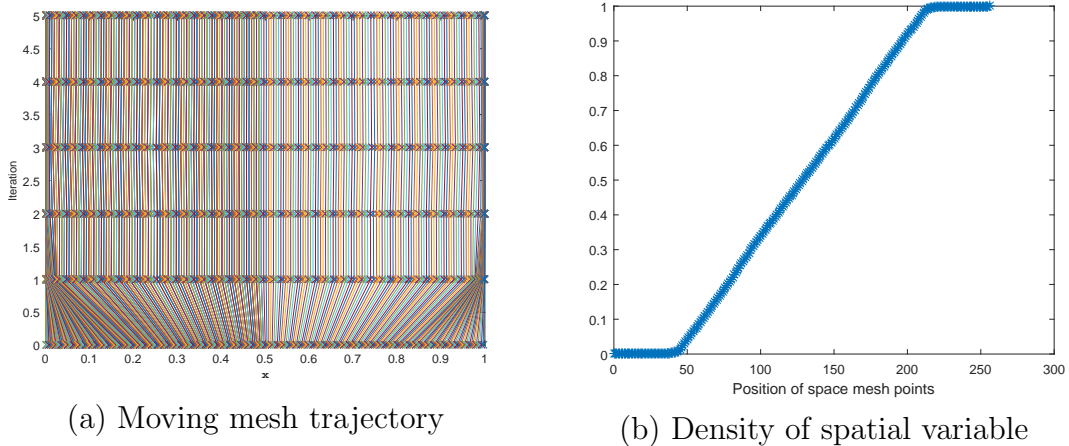


FIGURE 5.2: Mesh trajectory and final position of space mesh points with  $\varepsilon = 10^{-7}$  and  $N = 256$  for Example 5.5.1.

TABLE 5.1: Errors  $E^{\varepsilon,N,M}$ ,  $E^{N,M}$  and rates of convergence  $F^{\varepsilon,N,M}$ ,  $F^{N,M}$  using scheme (5.31) without Richardson extrapolation for Example 5.5.1.

$\varepsilon$	$N = 128$ $M = 4$	$N = 256$ $M = 8$	$N = 512$ $M = 16$	$N = 1024$ $M = 32$	$N = 2048$ $M = 64$
$10^0 = 1$	5.47E-03	2.97E-03	1.56E-03	7.99E-04	4.05E-04
	0.88	0.93	0.96	0.97	
$10^{-1}$	6.67E-03	3.52E-03	1.80E-03	9.15E-04	4.61E-04
	0.93	0.96	0.98	0.99	
$10^{-2}$	1.72E-02	9.08E-03	4.68E-03	2.38E-03	1.20E-03
	0.92	0.96	0.98	0.99	
$10^{-3}$	3.35E-02	1.76E-02	9.02E-03	4.57E-03	2.30E-03
	0.93	0.96	0.98	0.99	
$10^{-4}$	3.97E-02	2.08E-02	1.07E-02	5.39E-03	2.71E-03
	0.93	0.96	0.98	0.99	
$10^{-5}$	4.12E-02	2.16E-02	1.11E-02	5.61E-03	2.82E-03
	0.93	0.96	0.98	0.99	
$10^{-6}$	4.16E-02	2.18E-02	1.12E-02	5.66E-03	2.85E-03
	0.93	0.96	0.98	0.99	
$10^{-7}$	4.17E-02	2.18E-02	1.12E-02	5.67E-03	2.85E-03
	0.93	0.96	0.98	0.99	
$10^{-8}$	4.17E-02	2.18E-02	1.12E-02	5.67E-03	2.85E-03
	0.93	0.96	0.98	0.99	
$E^{N,M}$	4.17E-02	2.18E-02	1.12E-02	5.67E-03	2.85E-03
$F^{N,M}$	0.93	.96	0.98	0.99	

In Table 5.1, we have presented the maximum pointwise errors and the corresponding rates of convergence for the numerical solution computed by the algorithm given above for different values of the perturbation parameter and the discretization parameters in space ( $N$ ) and time ( $M$ ) varying with the same ratio ( $N$  and  $M$  both multiplied by 2) without using the Richardson extrapolation in time. In Tables 5.2 and 5.3, the solutions are computed by the above algorithm using extrapolation in time; taking the discretization parameters  $N$  and  $M$  multiplied by 2 in earlier, and



TABLE 5.2: Errors  $E^{\varepsilon,N,M}$ ,  $E^{N,M}$  and rates of convergence  $F^{\varepsilon,N,M}$ ,  $F^{N,M}$  using scheme (5.31) with Richardson extrapolation for Example 5.5.1.

$\varepsilon$	$N = 128$ $M = 4$	$N = 256$ $M = 8$	$N = 512$ $M = 16$	$N = 1024$ $M = 32$	$N = 2048$ $M = 64$
$10^0 = 1$	5.87E-04	2.74E-04	8.70E-05	2.65E-05	7.28E-06
	1.10	1.66	1.71	1.87	
$10^{-1}$	5.26E-04	1.62E-04	4.78E-05	1.31E-05	3.45E-06
	1.70	1.76	1.87	1.93	
$10^{-2}$	1.12E-03	3.23E-04	8.88E-05	2.33E-05	5.96E-06
	1.79	1.86	1.93	1.97	
$10^{-3}$	1.82E-03	5.18E-04	1.37E-04	3.55E-05	9.03E-06
	1.81	1.91	1.95	1.98	
$10^{-4}$	2.09E-03	5.79E-04	1.53E-04	3.94E-05	9.99E-06
	1.85	1.92	1.96	1.98	
$10^{-5}$	2.15E-03	5.94E-04	1.57E-04	4.04E-05	1.02E-05
	1.86	1.92	1.96	1.98	
$10^{-6}$	2.17E-03	5.97E-04	1.58E-04	4.06E-05	1.03E-05
	1.86	1.92	1.96	1.98	
$10^{-7}$	2.17E-03	5.98E-04	1.58E-04	4.06E-05	1.03E-05
	1.86	1.92	1.96	1.98	
$10^{-8}$	2.17E-03	5.98E-04	1.58E-04	4.06E-05	1.03E-05
	1.86	1.92	1.96	1.98	
$E^{N,M}$	2.17E-03	5.98E-04	1.58E-04	4.06E-05	1.03E-05
$F^{N,M}$	1.86	1.92	1.96	1.98	

$N$  multiplied by 2 and  $M$  multiplied by 4 in later to compute the rates of convergence. In each table, the last two rows represent the uniform errors and uniform rates of convergence.

In Table 5.2, the second order convergence is seen which is because of the time discretization error dominance in the global error over the space discretization error for this problem. The fourth order convergence results shown in Table 5.3 clearly confirms this assertion. Also, from these tables, we can conclude the improvement in rate of convergence using the Richardson extrapolation technique. In Table 5.3

TABLE 5.3: Errors  $E^{\varepsilon,N,M}$ ,  $E^{N,M}$  and rates of convergence  $\widehat{F}^{\varepsilon,N,M}$ ,  $\widehat{F}^{N,M}$  using scheme (5.31) with Richardson extrapolation for Example 5.5.1.

$\varepsilon$	$N = 128$ $M = 4$	$N = 256$ $M = 16$	$N = 512$ $M = 64$	$N = 1024$ $M = 256$	$N = 2048$ $M = 1024$
$10^0 = 1$	5.87E-04	8.70E-05	7.28E-06	4.92E-07	3.14E-08
	2.75	3.58	3.89	3.97	
$10^{-1}$	5.26E-04	4.78E-05	3.45E-06	2.25E-07	1.43E-08
	3.46	3.79	3.94	3.98	
$10^{-2}$	1.12E-03	8.88E-05	5.96E-06	3.79E-07	2.38E-08
	3.65	3.90	3.97	3.99	
$10^{-3}$	1.82E-03	1.37E-04	9.03E-06	5.71E-07	3.58E-08
	3.72	3.93	3.98	4.00	
$10^{-4}$	2.09E-03	1.53E-04	9.99E-06	6.32E-07	3.96E-08
	3.78	3.94	3.98	4.00	
$10^{-5}$	2.15E-03	1.57E-04	1.02E-05	6.46E-07	4.05E-08
	3.78	3.94	3.98	4.00	
$10^{-6}$	2.17E-03	1.58E-04	1.03E-05	6.50E-07	4.07E-08
	3.78	3.94	3.99	4.00	
$10^{-7}$	2.17E-03	1.58E-04	1.03E-05	6.50E-07	4.08E-08
	3.78	3.94	3.99	4.00	
$10^{-8}$	2.17E-03	1.58E-04	1.03E-05	6.50E-07	4.08E-08
	3.78	3.94	3.99	4.00	
$E^{N,M}$	2.17E-03	1.58E-04	1.03E-05	6.50E-07	4.08E-08
$\widehat{F}^{N,M}$	3.78	3.94	3.99	4.00	

we use the following formulas for orders of convergence

$$\widehat{F}^{\varepsilon,N,M} = \log_2 \left( \frac{E^{\varepsilon,N,M}}{E^{\varepsilon,2N,4M}} \right) \quad \text{and} \quad \widehat{F}^{N,M} = \log_2 \left( \frac{E^{N,M}}{E^{2N,4M}} \right).$$

In addition, the adaptive movement of mesh points towards the boundary layers and the heavy density of mesh points in layer regions are shown in Figure 5.2. In Figure 5.3, we have plotted the log-log graph between maximum pointwise error and the space discretization parameter  $N$  for the comparative convergence behavior of the

TABLE 5.4: Errors  $E^{\varepsilon,N,M}$ ,  $E^{N,M}$ , and rates of convergence  $F^{\varepsilon,N,M}$ ,  $F^{N,M}$  using scheme (5.31) without Richardson extrapolation for Example 5.5.2.

$\varepsilon$	$N = 128$ $M = 4$	$N = 256$ $M = 8$	$N = 512$ $M = 16$	$N = 1024$ $M = 32$	$N = 2048$ $M = 64$
$10^0 = 1$	6.79E-03	5.51E-03	3.51E-03	2.08E-03	1.14E-03
	0.30	0.65	0.76	0.86	
$10^{-1}$	1.71E-02	9.64E-03	5.14E-03	2.66E-03	1.35E-03
	0.83	0.91	0.95	0.95	
$10^{-2}$	2.63E-02	1.50E-02	8.02E-03	4.16E-03	2.12E-03
	0.81	0.90	0.95	0.97	
$10^{-3}$	2.76E-02	1.57E-02	8.45E-03	4.39E-03	2.23E-03
	0.81	0.90	0.95	0.97	
$10^{-4}$	2.77E-02	1.58E-02	8.50E-03	4.41E-03	2.25E-03
	0.81	0.89	0.94	0.97	
$10^{-5}$	2.77E-02	1.58E-02	8.50E-03	4.41E-03	2.25E-03
	0.81	0.89	0.94	0.97	
$10^{-6}$	2.77E-02	1.58E-02	8.50E-03	4.41E-03	2.25E-03
	0.81	0.89	0.94	0.97	
$10^{-7}$	2.77E-02	1.58E-02	8.50E-03	4.41E-03	2.25E-03
	0.81	0.89	0.94	0.97	
$10^{-8}$	2.77E-02	1.58E-02	8.50E-03	4.41E-03	2.25E-03
	0.81	0.89	0.94	0.97	
$E^{N,M}$	2.77E-02	1.58E-02	8.50E-03	4.41E-03	2.25E-03
$F^{N,M}$	0.81	0.89	0.94	0.97	

scheme (5.31) with and without the Richardson extrapolation for two values of  $\varepsilon$  and for different discretization parameter ratios between space and time variables. Here, from the slopes of these plots we can clearly see that for Example 5.5.1 the rate of convergence of the scheme (5.31) is increased to second order from first on using the Richardson extrapolation technique. Certainly, these results highly validate the theoretical results.

TABLE 5.5: Errors  $E^{\varepsilon,N,M}$ ,  $E^{N,M}$  and rates of convergence  $F^{\varepsilon,N,M}$ ,  $F^{N,M}$  using scheme (5.31) with Richardson extrapolation for Example 5.5.2.

$\varepsilon$	$N = 128$ $M = 4$	$N = 256$ $M = 8$	$N = 512$ $M = 16$	$N = 1024$ $M = 32$	$N = 2048$ $M = 64$
$10^0 = 1$	1.40E-03	1.51E-03	6.78E-04	2.23E-04	6.51E-05
	1.12	1.16	1.60	1.78	
$10^{-1}$	2.19E-03	6.51E-04	1.79E-04	6.51E-05	1.21E-05
	1.75	1.86	1.46	2.42	
$10^{-2}$	3.63E-03	1.09E-03	3.01E-04	7.92E-05	2.03E-05
	1.73	1.86	1.93	1.96	
$10^{-3}$	3.88E-03	1.17E-03	3.23E-04	8.51E-05	2.18E-05
	1.73	1.86	1.93	1.96	
$10^{-4}$	3.90E-03	1.18E-03	3.26E-04	8.57E-05	2.20E-05
	1.73	1.86	1.93	1.96	
$10^{-5}$	3.90E-03	1.18E-03	3.26E-04	8.57E-05	2.20E-05
	1.73	1.86	1.93	1.96	
$10^{-6}$	3.90E-03	1.18E-03	3.26E-04	8.57E-05	2.20E-05
	1.73	1.86	1.93	1.96	
$10^{-7}$	3.90E-03	1.18E-03	3.26E-04	8.57E-05	2.20E-05
	1.73	1.86	1.93	1.96	
$10^{-8}$	3.90E-03	1.18E-03	3.26E-04	8.57E-05	2.20E-05
	1.73	1.86	1.93	1.96	
$E^{N,M}$	3.90E-03	1.18E-03	3.26E-04	8.57E-05	2.20E-05
$F^{N,M}$	1.73	1.86	1.93	1.96	

Example 5.5.2. Consider the problem [88]

$$\begin{cases} \frac{\partial y}{\partial t} - \varepsilon \frac{\partial^2 y}{\partial x^2} + (1 + x^2 + t^2 e^t)y = e^t - 1 + \sin(\pi x), & (x, t) \in G, \\ y(x, 0) = 0, \quad x \in \bar{G}_x, \quad y(0, t) = 0, \quad y(1, t) = 0, \quad t \in (0, T]. \end{cases} \quad (5.35)$$

For this test example we do not know the exact solution. Therefore, for numerical errors and rates of convergence we shall use a variant of the double mesh principle. For this purpose we bisect the spatial mesh into  $2N$  intervals and the time mesh

TABLE 5.6: Errors  $E^{\varepsilon,N,M}$ ,  $E^{N,M}$  and rates of convergence  $\widehat{F}^{\varepsilon,N,M}$ ,  $\widehat{F}^{N,M}$  using scheme (5.31) with Richardson extrapolation for Example 5.5.2.

$\varepsilon$	$N = 128$ $M = 4$	$N = 256$ $M = 16$	$N = 512$ $M = 64$	$N = 1024$ $M = 256$	$N = 2048$ $M = 1024$
$10^0 = 1$	1.40E-03	6.78E-04	6.50E-05	4.61E-06	2.98E-07
	1.05	3.38	3.82	3.95	
$10^{-1}$	2.19E-03	1.79E-04	1.21E-05	7.73E-07	4.86E-08
	3.61	3.89	3.97	3.99	
$10^{-2}$	3.63E-03	3.01E-04	2.03E-05	1.29E-06	8.12E-08
	3.59	3.89	3.97	3.99	
$10^{-3}$	3.88E-03	3.23E-04	2.18E-05	1.39E-06	8.73E-08
	3.58	3.89	3.97	3.99	
$10^{-4}$	3.90E-03	3.26E-04	2.20E-05	1.40E-06	3.94E-08
	3.58	3.89	3.97	3.99	
$10^{-5}$	3.90E-03	3.26E-04	2.20E-05	1.40E-06	3.94E-08
	3.58	3.89	3.97	3.99	
$10^{-6}$	3.90E-03	3.26E-04	2.20E-05	1.40E-06	3.94E-08
	3.58	3.89	3.97	3.99	
$10^{-7}$	3.90E-03	3.26E-04	2.20E-05	1.40E-06	3.94E-08
	3.58	3.89	3.97	3.99	
$10^{-8}$	3.90E-03	3.26E-04	2.20E-05	1.40E-06	3.94E-08
	3.58	3.89	3.97	3.99	
$E^{N,M}$	3.90E-03	3.26E-04	2.20E-05	1.40E-06	3.94E-08
$\widehat{F}^{N,M}$	3.58	3.89	3.97	3.99	

into  $2M$  and  $4M$  intervals so that now the pointwise errors are calculated by

$$E_{i,n}^{\varepsilon,N,M} = |Y_i^{n,2N,2M} - Y_i^{n,N,M}|,$$

when scheme (5.31) is used, and

$$E_{i,n}^{\varepsilon,N,M} = |(2Y_i^{n,2N,4M} - Y_i^{n,2N,2M}) - (2Y_i^{n,N,2M} - Y_i^{n,N,M})|,$$

TABLE 5.7: Errors  $E^{\varepsilon,N,M}$ ,  $E^{N,M}$  and rates of convergence  $F^{\varepsilon,N,M}$ ,  $F^{N,M}$  using scheme (5.31) without Richardson extrapolation for Example 5.5.3.

$\varepsilon$	$N = 128$ $M = 4$	$N = 256$ $M = 8$	$N = 512$ $M = 16$	$N = 1024$ $M = 32$	$N = 2048$ $M = 64$
$10^0 = 1$	6.60E-08 3.96	4.24E-09 4.11	2.45E-10 4.10	1.43E-11 3.37	1.39E-12
$10^{-1}$	3.35E-08 4.14	1.90E-09 4.24	1.01E-10 3.82	7.10E-12 4.17	3.95E-13
$10^{-2}$	1.50E-07 4.40	7.14E-09 4.04	4.35E-10 3.62	3.55E-11 3.79	2.56E-12
$10^{-3}$	2.10E-06 4.55	9.00E-08 4.24	4.77E-09 3.69	3.70E-10 3.42	3.45E-11
$10^{-4}$	8.34E-06 4.43	3.86E-07 4.34	1.90E-08 3.52	1.66E-09 4.20	9.06E-11
$10^{-5}$	1.05E-05 4.08	6.16E-07 4.15	3.46E-08 3.68	2.69E-09 4.00	1.69E-10
$10^{-6}$	1.77E-05 4.41	8.33E-07 4.34	4.11E-08 3.77	3.02E-09 3.86	2.08E-10
$10^{-7}$	1.72E-05 4.05	1.04E-06 4.41	4.92E-08 3.96	3.17E-09 3.50	2.81E-10
$10^{-8}$	1.67E-05 4.34	8.23E-07 4.09	4.83E-08 3.74	3.62E-09 3.86	2.49E-10
$E^{N,M}$	1.77E-05	8.33E-07	4.92E-08	3.62E-09	2.81E-10
$F^{N,M}$	4.40	4.08	3.76	3.69	

when scheme (5.31) is used with extrapolation technique (5.33). Using these values, maximum errors for each value of  $\varepsilon$  and the rates of convergence are calculated by

$$E^{\varepsilon,N,M} = \max_{i,n} E_{i,n}^{\varepsilon,N,M}, \quad F^{\varepsilon,N,M} = \log_2 \left( \frac{E^{\varepsilon,N,M}}{E^{\varepsilon,2N,2M}} \right).$$

TABLE 5.8: Errors  $E^{\varepsilon,N,M}$ ,  $E^{N,M}$  and rates of convergence  $F^{\varepsilon,N,M}$ ,  $F^{N,M}$  using scheme (5.31) with Richardson extrapolation for Example 5.5.3.

$\varepsilon$	$N = 128$ $M = 4$	$N = 256$ $M = 8$	$N = 512$ $M = 16$	$N = 1024$ $M = 32$	$N = 2048$ $M = 64$
$10^0 = 1$	6.59E-08 3.96	4.24E-09 4.11	2.45E-10 4.11	1.42E-11 1.44	5.20E-12
$10^{-1}$	3.25E-08 4.12	1.87E-09 4.23	9.97E-11 3.83	7.00E-12 3.27	7.26E-13
$10^{-2}$	1.50E-07 4.40	7.14E-09 4.04	4.35E-10 3.62	3.55E-11 3.79	2.56E-12
$10^{-3}$	2.10E-06 4.54	9.00E-08 4.24	4.77E-09 3.69	3.70E-10 3.42	3.45E-11
$10^{-4}$	8.32E-06 4.43	3.86E-07 4.34	1.90E-08 3.52	1.66E-09 4.20	9.06E-11
$10^{-5}$	1.04E-05 4.08	6.16E-07 4.15	3.46E-08 3.68	2.69E-09 4.00	1.69E-10
$10^{-6}$	1.76E-05 4.40	8.33E-07 4.34	4.11E-08 3.77	3.02E-09 3.86	2.08e-10
$10^{-7}$	1.72E-05 4.04	1.04E-06 4.41	4.92E-08 3.96	3.17E-09 3.50	2.81e-10
$10^{-8}$	1.67E-05 4.34	8.23E-07 4.09	4.83E-08 3.74	3.62E-09 3.86	2.49E-10
$E^{N,M}$	1.76E-05	8.33E-07	4.92E-08	3.62E-09	2.81e-10
$F^{N,M}$	4.40	4.08	3.76	3.69	

Then the parameter-robust errors and parameter-robust rates of convergence over the set of  $\varepsilon$  are obtained by

$$E^{N,M} = \max_{\varepsilon} F^{\varepsilon,N,M}, \quad F^{N,M} = \log_2 \left( \frac{E^{N,M}}{E^{2N,2M}} \right).$$

Figure 5.4 displays the numerical solution of Example 5.5.2 for  $\varepsilon = 10^{-5}$ . Again, we observe the boundary layers at  $x = 0$  and  $x = 1$ . From Tables 5.4 and 5.5, we see that the order of parameter-robust convergence of the discretization scheme (5.31)

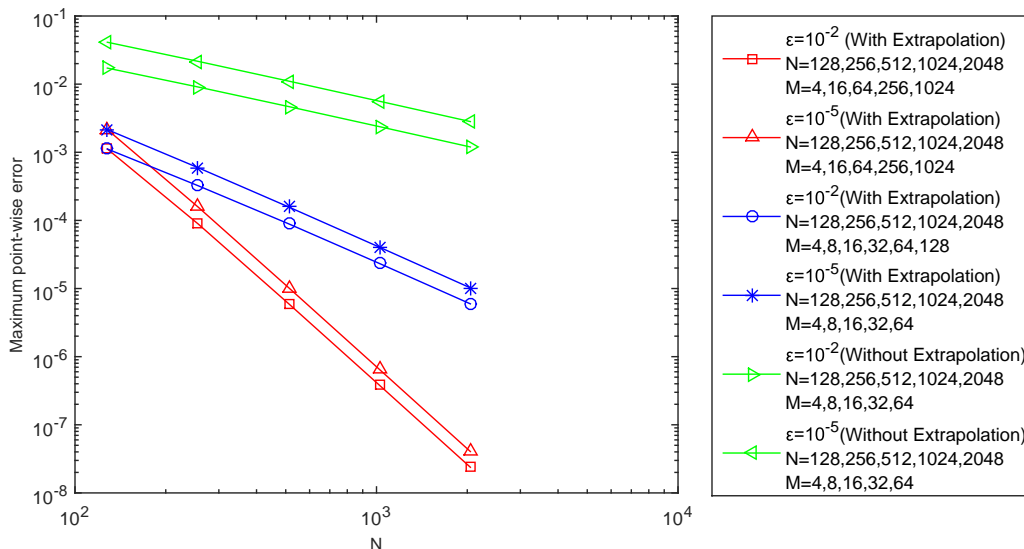


FIGURE 5.3: Log-log plot for maximum error vs  $N$  for Example 5.5.1.

is increased from first to second order on using the Richardson extrapolation in time. Also, Tables 5.5 and 5.6 show the orders of convergence of the discretization scheme (5.31) with the Richardson extrapolation in time when the discretization parameter in time ( $M$ ) is doubled and quadrupled, respectively. Clearly, these numerical results are in good agreement with the theoretical results. In Table 5.6 the orders of convergence are computed using the formulas as defined for Table 5.3.

*Example 5.5.3.* Consider the problem [87]

$$\begin{cases} \frac{\partial y}{\partial t} - \varepsilon \frac{\partial^2 y}{\partial x^2} + (1 + xe^{-t})y = f(x, t), & (x, t) \in G, \\ y(x, 0) = 0, \quad x \in \bar{G}_x, \quad y(0, t) = 0, \quad y(1, t) = 0, \quad t \in (0, T], \end{cases} \quad (5.36)$$

with the term  $f(x, t)$  taken according to the exact solution given by

$$y(x, t) = t \left( \frac{e^{-\frac{x}{\sqrt{\varepsilon}}} + e^{-\frac{-(1-x)}{\sqrt{\varepsilon}}}}{1 + e^{-\frac{1}{\sqrt{\varepsilon}}}} - \cos^2(\pi x) \right).$$



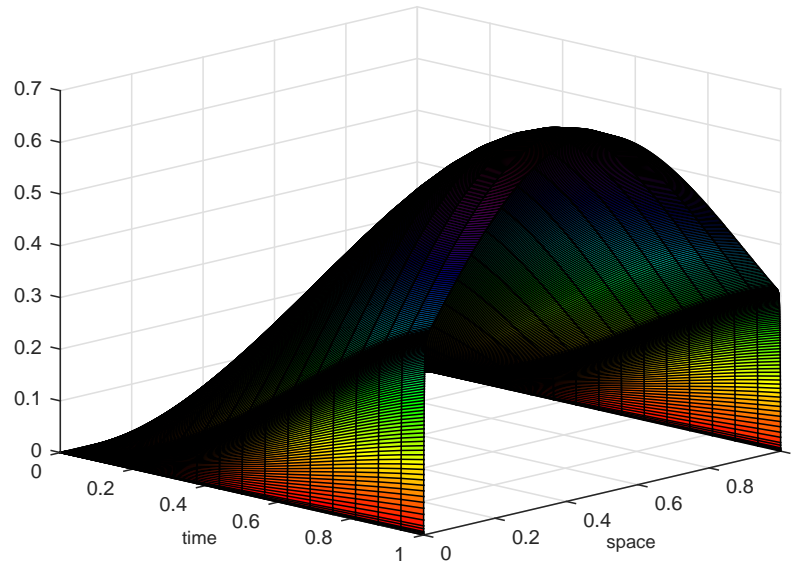


FIGURE 5.4: Surface plot of numerical solution of Example 5.5.2 for  $\varepsilon = 10^{-5}$ ,  $N = 512$ , and  $M = 16$ .

For this problem we have the exact solution, so for the pointwise errors, maximum errors and parameter-robust rates of convergence we can use the same formulas as defined for Example 5.5.1. Similarly, the parameter-robust errors and parameter-robust rates of convergence are calculated. In this problem the contribution of the error corresponding the time discretization to the global error is negligible. That is why even without the Richardson extrapolation in time we are getting the fourth order convergence as shown in Table 5.7. In Table 5.8, the maximum pointwise errors and rates of convergence are shown for the scheme (5.31) with the Richardson extrapolation in time. So, for this test example, the results also authenticate the validity of the theoretical results.

## 5.6 Conclusions

We presented a high order parameter-robust convergent adaptive numerical method for singularly perturbed time dependent reaction-diffusion problems. The problem is discretized firstly in time using the implicit Euler scheme on a uniform mesh. Then the obtained semidiscrete problems are discretized in space using a non-monotone finite difference scheme. After that the totally discrete scheme is defined and it is proved to be convergent of order one in time and four in space, independent of the perturbation parameter. Further, the Richardson extrapolation technique is applied to improve the order of convergence in time from one to two. Numerical results are given in support of the theory.

\*\*\*\*\*